Developmental Biology **250,** 305–316 (2002)
doi:10.1006/dbio.2002.0807

# Affinity Regulates Spatial Range of EGF Receptor Autocrine Ligand Binding

**Ann DeWitt,* Tomoko Iida,* Ho-Yan Lam,* Virginia Hill,† H. Steven Wiley,‡ and Douglas A. Lauffenburger*,§,[1]**

**Department of Chemical Engineering,* §*Biological Engineering Division, Department of Biology, and Center for Cancer Research, Massachusetts Institute of Technology, Cambridge, Massachusetts 02139;* †*Division of Cell Biology and Immunology, Department of Pathology, University of Utah Medical School, Salt Lake City, Utah; and* ‡*Fundamental Sciences Division, Pacific Northwest National Laboratory, Richland, Washington 99352*

**Proper spatial localization of EGFR signaling activated by autocrine ligands represents a critical factor in embryonic development as well as tissue organization and function, and ligand/receptor binding affinity is among the molecular and cellular properties suggested to play a role in governing this localization. We employ a computational model to predict how receptor-binding affinity affects local capture of autocrine ligand *vis-a-vis* escape to distal regions, and provide experimental test by constructing cell lines expressing EGFR along with either wild-type EGF or a low-affinity mutant, $EGF^{L47M}$. The model predicts local capture of a lower affinity autocrine ligand to be less efficient when the ligand production rate is small relative to receptor appearance rate. Our experimental data confirm this prediction, demonstrating that cells can use ligand/receptor binding affinity to regulate ligand spatial distribution when autocrine ligand production is limiting for receptor signaling.** 

## INTRODUCTION

EGFR[2] signaling activated by autocrine ligands is crucially involved in many physiological processes, such as mammary (Li *et al.,* 1992; Panico *et al.,* 1996; Wiesen *et al.,* 1999), prostate (Kim *et al.,* 1999), and skeletal tissue organization (Miettinen *et al.,* 1999), wound healing (Piepkorn *et al.,* 1998), and liver homeostasis (Chung *et al.,* 2000; Hisaka *et al.,* 1999; Russell *et al.,* 1993). Moreover, the importance of the spatial distribution of EGFR signaling in embryonic development has been demonstrated in a variety of model organisms (Bier, 1998; Horvitz and Sternberg, 1991; Kornfeld, 1997; Schweitzer and Shilo, 1997; Wasserman and Freeman, 1997).

As one example, a number of processes in *Drosophila* embryogenesis are governed by highly regulated and spatially localized autocrine and paracrine ligands that bind the *Drosophila* EGFR, DER (Schweitzer and Shilo, 1997). DER along with Spitz, a DER ligand processed as a transmembrane protein and subsequently cleaved to activate DER, are ubiquitously expressed in embryo development, but DER activation via binding of Spitz is modulated for diverse effects (Bier, 1998; Wasserman and Freeman, 1997). Processing of the transmembrane Spitz precursor into its secreted form is mediated by the chaparone Star in conjunction with the protease Rhomboid (Klambt, 2002). A second secreted DER ligand, Argos, can further modulate DER signaling patterns by competitively inhibiting DER activation (Schweitzer *et al.,* 1995; Jin *et al.,* 2000). Argos appears to exhibit more distal effects than does Spitz (Freeman, 1997; Gabay *et al.,* 1997); Spitz has been recently demonstrated to remain highly localized to its point of release (Bergmann *et al.,* 2002). During patterning of the ventral ectoderm, Rhomboid is expressed only in midline cells (Golembo *et al.,* 1996); Spitz accordingly originates in the midline and activates DER locally (Gabay *et al.,* 1997; Wasserman and Freeman, 1997). Ectopic expression of secreted Spitz or Rhomboid in the ectoderm or mesoderm results in ventralization of the embryo (Golembo *et al.,* 1996), and Argos mutant embryos also show an expanded

[1] To whom correspondence should be addressed. Fax: (617) 258-0204. E-mail: lauffen@mit.edu.

[2] Abbreviations used: EGFR, epidermal growth factor receptor; EGF, epidermal growth factor; DER, *Drosophila* EGF receptor; TGFα, transforming growth factor alpha; AR, amphiregulin; DMEM, Dulbecco's Modified Eagle Medium; mAb, monoclonal antibody; PBS, phosphate buffered saline; DCS, dialyzed calf serum; BSA, bovine serum albumin; WT, wild-type.

0012-1606/02 $35.00

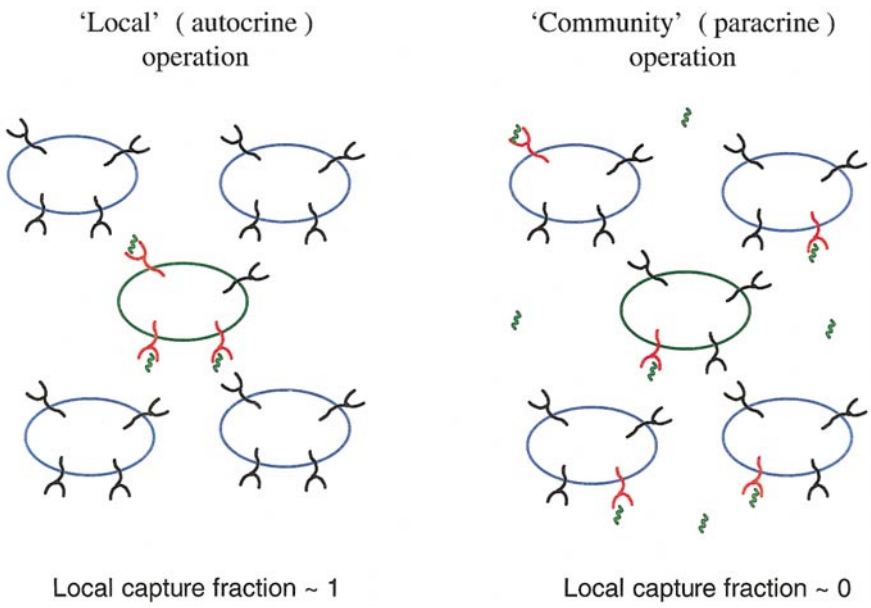


**FIG. 1.** Illustration of autocrine vs paracrine ligand signaling. Green cells (center) produce ligand and express corresponding receptor; blue cells (surrounding) do not produce ligand but express receptor. Black receptors are unoccupied by ligand; red receptors are bound by ligand. (Left) Case of pure autocrine (or, "local") operation, with essentially all ligand captured by producing cell. (Right) Case of paracrine (or, "community") operation, with very little ligand captured by producing cell.

region of ventralization (Gabay *et al.*, 1997). The difference between spatial ranges of Spitz and Argos, leading to proximal vs distal effects on DER activity, has been hypothesized to contribute to the formation of pair dorsal appendages (Wasserman and Freeman, 1998); this hypothesis is supported by a recent computational modeling analysis (Shvartsman *et al.*, 2002).

Similar, but more poorly understood, localization-dependent effects on DER signaling resulting from competition between activating and inhibitory secreted autocrine ligands may be occurring in organization of the fly eye imaginal disk (Gabay *et al.*, 1997; Baonza *et al.*, 2001). Moreover, spatially restricted autocrine/paracrine signaling in the *Cacnorhabditis elegans* lin-3/let-23 system, the worm EGF/EGFR system homologue, may be crucially involved in coordinated uterus and vulva development (Chang *et al.*, 1999). More broadly yet, mouse mammary gland development is dependent on autocrine EGFR signaling (Schroeder and Lee, 1998), in a manner that appears to be strongly influenced by the ligand identity among EGF, TGF$\alpha$, and AR (Luetteke *et al.*, 1999).

These findings motivate investigation of molecular and cellular properties which determine the spread of autocrine ligand before receptor capture, especially for the EGFR system. Previous theoretical work has offered a set of properties which might do so, including ligand diffusivity, receptor expression level, ligand/receptor binding affinity, and ligand/receptor complex endocytic trafficking rate constants (Shvartsman *et al.*, 2001). The same properties have been similarly indicated by analogous theoretical treatment of paracrine factors in formation of morphogen gradients for developmental regulation (Lander *et al.*, 2002). An experimental study of localized autocrine ligand capture for an EGF-producing cell line in culture has verified the effect of EGFR expression level, showing that the fraction of ligand captured proximally by producing cells falls from nearly 1 to nearly 0 as the ratio of ligand release rate to receptor synthesis rate increases (DeWitt *et al.*, 2001). A proximal capture fraction near 1 corresponds to pure autocrine signaling, or "local" operation, whereas a proximal capture fraction near 0 corresponds to mostly paracrine signaling, or "community" operation (see Fig. 1).

However, the effects of ligand properties such as receptor-binding affinity on autocrine ligand spatial range have not yet been examined, to our knowledge. Because multiple ligands exist in the EGF family for most organisms (Moghal and Sternberg, 1999; Yarden, 2001) and exhibit diverse receptor-binding properties (Shoyab *et al.*, 1989; Derynck, 1992; Chung and Coffey, 2000; Iwamoto and Mekada, 2000), this represents an important property to consider for its potential role in regulating spatial distribution of EGFR signaling.

Thus, the question we pose here is: can differences in EGFR-binding affinity lead to corresponding differences in spatial localization of autocrine EGF ligands? We start from our recent analysis of the EGFR autocrine system in engineered B82 mouse fibroblasts (DeWitt *et al.*, 2001), measuring the fraction of WT EGF autocrine ligand captured locally and the associated fraction of occupied EGFR, enabling us to validate a computational model describing this

system. We then employ this model to generate *a priori* prediction of how altering ligand/receptor binding affinity should affect the fraction of occupied EGFR and the fraction of EGF autocrine ligand captured locally. The model predicts that a low-affinity autocrine system will be less efficient at capturing ligand locally, compared with a higher affinity counterpart, at low but not high ligand production rates relative to receptor production rates. To test our predictions, we generate a novel low-affinity EGF mutant by making a single-amino acid substitution in EGF, Leu 47 to Met, possessing an approximately eightfold lower binding affinity for the EGFR compared with wild-type EGF; this mutation is motivated by its critical role in the lower AR binding affinity (Adam *et al.*, 1995). The experimental data are in agreement with the model predictions, thus showing that cells can regulate the spatial range of autocrine EGFR loops not only through processes controlling ligand release and receptor expression but also by those modulating the binding affinity of the receptor/ligand pair.

## MATERIALS AND METHODS

### *Construction of Mutant EGF$^{L47M}$ Gene*

A low-affinity form of human EGF was constructed by using a trunctated form of the EGF gene, EGF-Ct, described elsewhere (Wiley *et al.*, 1998). EGF-Ct contains a signal sequence, the mature ligand sequence, as well as the transmembane and cytoplasmic domains. The gene is in pBluescript with *Not*I and *Bam*HI sites flanking the gene 5′ and 3′, respectively. Two PCR primers were constructed to introduce two-point mutations converting the nucleotides corresponding to leucine[47] of the mature ligand to encode for methionine (5′-CAG TAC CGA GAT ATG AAG TGG TGG GAA-3′ and 5′-TTC CCA CCA CTT CAT ATC TCG GTA CTG-3′). The primers were used in conjunction with T7 and T3 primers, which anneal to sequences flanking the multiple cloning site of pBluescript, to generate overlapping primary PCR products. The final PCR product was amplified by using T7 and T3 primers. The construct was verified by DNA sequencing. The PCR product containing the mutant EGF gene was then ligated into the pIRESpuro vector (CLONTECH Laboratories, Inc., Palo Alto, CA) after digestion with *Not*I and *Bam*HI. The construct was again verified by DNA sequencing.

### *Production and Purification of EGF$^{L47M}$*

Chinese hamster ovary cells, W3 ATCC, were cultured in a mixture containing 5% HAM's F12 and MEM-$\alpha$ supplemented with 5% certified fetal calf serum (all from Gibco) and 5% defined supplemented calf serum (HyClone Laboratories, Inc., Logan, UT) and 95% SFX-CHO media (HyClone). Cells were transfected with pIRESpuro-EGF$^{L47M}$ using LipofectAMINE reagent (Gibco). After transfection, the medium was supplemented with 40 $\mu$g/ml puromycin to select transfected cells (CLONTECH Laboratories, Inc.). We isolated CHO cells expressing higher levels of EGF$^{L47M}$ by FAC sorting using anti-EGF antibody Z-12 (Santa Cruz Biotechnology, Inc., Santa Cruz, CA) and anti-rabbit IgG antibody conjugated to Alexa488 (Molecular Probes, Inc., Eugene, OR). The FACS CHO-EGF$^{L47M}$ cells were grown in suspension in spinner flasks for 7–10 days. The conditioned media was collected, filtered through a 0.2-$\mu$m nitrocellulose membrane, and then concentrated by using ultracentifugation devices (Centricon Plus-80, Millipore) with a 5000 nominal molecular weight cut-off. The concentrated retentate was then frozen at −20°C until antibody affinity chromatography.

Anti-EGF monoclocal antibodies LB and LC were conjugated to cyanogenbromide-activated sepharose beads and stored in PBS with 0.02% Azide until use. The concentrated retentate was added to the conjugated beads and rocked overnight at 4°C in slurry. The slurry was then loaded into a column (0.8 × 20 cm) and rinsed with 20 bed volumes of running buffer (PBS). The protein was eluted with an acid strip (100 mM glycine, 100 mM NaCl at pH 2.5) and collected in fractions containing 5% collection buffer (3.6 M NaCl, 81 mM KCl, 0.3 M phosphate buffer at pH 8.0). The fractions were concentrated by using ultracentifugation devices (Centriplus, Millipore) with a 3000 nominal molecular weight cut-off and tested by ELISA for concentration of EGF$^{L47M}$.

SDS-PAGE for was used to confirm the size of the mutant protein. Precast Tris-Tricine gels designed for small proteins were prepared and run as described in the instructions using Tris-Tricine running buffer and sample buffer all purchased from Bio-Rad. Samples of $^{125}$I-EGF$^{L10M}$ and $^{125}$I-EGF were loaded into separate wells alongside polypeptide standards and run at 100 V for 90 min (same iodination procedure as described for EGF below). The gel was exposed for 2 h before imaging using a Bio-Rad Molecular Imager.

### *Autocrine Cells Expressing Mutant EGF$^{L47M}$*

Parental B82L mouse fibroblasts transfected with the human EGFR were a gift from Gordon Gill. The cells were grown in DMEM, 10% DCS (10,000 mol wt cutoff), penicillin, streptomycin, and 1 $\mu$M methotrexate (Sigma). The cells were transfected with pIRESpuro-EGF$^{L47M}$ using FuGENE 6 (Roche Molecular Biochemicals, Indianapolis, IN) and selected and grown using 4.0 $\mu$g/ml puromycin (CLONTECH Laboratories, Inc.). Clones were isolated and checked for EGF$^{L47M}$ expression by ELISA. We varied ligand secretion and thus the production ratio using clones secreting different amounts of EGF$^{L47M}$. We also isolated additional populations using flow cytometry and cells labeled with anti-EGF antibody Z-12 (Santa Cruz Biotechnology, Inc.) and anti-rabbit IgG antibody conjugated to Alexa488 (Molecular Probes, Inc.). In addition, we varied the production ratio via receptor appearance by FAC sorting the original population of B82 EGFR+ paracrine cells for various receptor expression levels using an anti-EGFR antibody 13A9 (Genentech) in combination with anti-mouse IgG antibody conjugated to Alexa488 (Molecular Probes, Inc.) before transfection with pIRESpuro-EGF$^{L47M}$.

### *Bulk Medium Conditioning and Microphysiometer Assays*

These two assays have been described elsewhere (DeWitt *et al.*, 2001). Briefly, for the bulk medium conditioning assay, parallel wells of cells were plated. On day 3, the medium was changed to medium without antibiotics and a given concentration of BB-3103. On day 4, the medium was switched to 1% DCS, a given concentration of BB-3103, and a given concentration of anti-EGFR blocking mAb 225. After the cells conditioned their medium for a given time (8–14 h), the medium was collected, and the concentration of EGF or EGF$^{L47M}$ was assayed by ELISA. The EGF sandwich ELISA has been described elsewhere (Will *et al.*, 1995).

Transwells for the microphysiometer were prepared as described previously. The transwells with autocrine EGF$^{L47M}$ cells were plated on the Cytosensor, and a baseline rate of extracellular acidification (ECAR) was established. Once the baseline was estab-

lished, the cells were challenged with a given concentration of exogenous EGF. A transwell was subjected to only one challenge before being discarded. The normalized, maximal change in the acidification rate (ECAR-Max) was recorded as a function of exogenous EGF concentration. Using an improved microphysiometer model, similar to a model previously described (DeWittt *et al.*, 2001), we determined the autocrine ligand concentration as a function of autocrine ligand secretion rate.

## *Determination of Binding Rate Constants*

Recombinant human EGF was obtained from PeproTech and iodinated with $^{125}$I (NEN Life Science Products) using IODOBEADS (Pierce) according to the manufacturer's recommendations. Free iodine was separated from radiolabeled protein by using a column (0.8 × 20 cm) packed with Sephadex G-10. The activity and concentration were determined by using pre-and postcolumn samples and a phosphotungstic acid precipitation.

On day 1, B82 EGFR+ cells were plated in 35-mm dishes at a 1:10 dilution. On day 3, the media was changed to Hepes-buffered DMEM, 1% DCS, 0.5 mg/ml BSA (D/H/B). On day 4, the plates were washed two times with cold saline (1 mg/ml polyvinyl pyrrolidone, 130 mM NaCl, 5 mM KCl, 0.5 mM $MgCl_2$–$6H_20$, 1 mM $CaCl_2$–$2H_2O$ 20 mM Hepes) and 0.2 mM phenylarsine oxide (PAO) in saline was added to each plate to inhibit internalization (Gibson *et al.*, 1989). The plates were then kept on ice for 20 min. After 20 min, the PAO solution was removed and 37°C D/H/B was added. The cells were incubated at 37°C with 1 nM $^{125}$I-EGF and with or without 60 ng/ml cold EGF$^{L47M}$ for times ranging from 1 to 7 min in duplicate. After a given time, plates were washed four times with cold saline, and the counts associated with the surface were determined by collecting supernant of an acid strip (50 mM glycine–HCl, 100 mM NaCl, 2 mg/ml polyvinyl pyrrolidone, 2 M urea, pH 3.0). In parallel, the total number of receptors on the cell surface was determined by generating an $^{125}$I-EGF equilibrium-binding curve.

The kinetic rate constants for EGF$^{L47M}$ were determined from plots of the fraction of total receptors occupied by labeled EGF in time for sample with and without cold EGF$^{L47M}$; two nonlinear equations describing receptor/ligand binding (Eqs. 1 and 2); and a MATLAB function designed to solve nonlinear curve-fitting problems. Equation 1 describes the time rate of change of the fraction of labeled surface complexes ($^{125}$I-EGF bound to EGFR); equation 2 describes the time rate of change of the fraction of unlabelled surface complexes (EGF$^{L47M}$ bound to EGFR). The assumptions embedded in these calculations are that the concentration of endogenous ligand does not change during the time course of the experiment and that no processes other than receptor/ligand binding (such as trafficking) are taking place.

$$\frac{df_{labeled}}{dt} = kon_{labeled} * L_{labeled} * (1 - f_{labeled} - f_{unlabeled}) - koff_{labeled} * f_{labeled} \quad [1]$$

$$\frac{df_{unlabeled}}{dt} = kon_{unlabeled} * L_{unlabeled} * (1 - f_{labeled} - f_{unlabeled}) - koff_{unlabeled} * f_{unlabeled}, \quad [2]$$

where $f_{labeled} = Cs_{labeled}/RsT$ and $f_{unlabeled} = Cs_{unlabeled}/RsT$; $Cs_{labeled}$ is the number of labeled receptor/ligand complexes, $Cs_{unlabeled}$ is the number of unlabeled receptor/ligand complexes, and RsT is the total number of receptors on the surface.

First, for one set of experiments, the association and dissociate rate constants of $^{125}$I-EGF were calculated from $^{125}$I-EGF-only transient data. Then, the association and dissociation rate constants of EGF$^{L47M}$ were calculated by using the previously calculated rate constants for $^{125}$I-EGF in conjunction with the $^{125}$I-EGF with cold EGF$^{L47M}$ transient data. Calculations for the association and dissociation rate constants were based on five sets of independent experiments.

## *Computational Autocrine Cell Model*

We describe here a computational autocrine cell model which consists of three parts: (1) system of equations describing autocrine receptor and ligand binding and trafficking, (2) calculation of fraction receptor occupied, $f_{R\ occupied}$, and (3) rate balance to calculate fraction ligand capture, $f_{LC}$. First, we solved a system of equations describing autocrine receptor and ligand binding and trafficking at steady state to calculate $f_{R\ occupied}$. Equations 3 and 4 describe the time rate of change of the number of endogenous complexes on the surface and inside the cell, respectively. Equations 5 and 6 describe the time rate of change of free surface receptors and total internal receptors, respectively. The parameter values and how these values are determined are listed and described elsewhere (DeWitt *et al.*, 2001). An important input for this model is the autocrine ligand concentration, $L_{auto}$, which is known as a function of $V_{LT}$, from previous work on the WT EGF/EGFR system (DeWitt *et al.*, 2001) and is validated in this work for the low-affinity EGF$^{L47M}$ autocrine system.

$$\frac{dCs_{auto}}{dt} = kon_{auto} * Rs * L_{auto} - koff_{auto} * Cs_{auto} - k_{eC} * Cs_{auto} \quad [3]$$

$$\frac{dRs}{dt} = -kon_{auto} * Rs * L_{auto} + koff_{auto} * Cs_{auto} - k_{eR} * Rs + k_{rec} * (1 - fR) * RiT + V_s \quad [4]$$

$$\frac{dCi_{auto}}{dt} = k_{eC} * Cs_{auto} - [k_{rec} * (1 - fR) + k_{dgr} * fR] * Ci_{auto} \quad [5]$$

$$\frac{dRiT}{dt} = k_{eR} * Rs + k_{eC} * Cs_{auto} - [k_{rec} * (1 - fR) + k_{dgr} * fR] * RiT, \quad [6]$$

where $kon_{auto}$ is the association rate constant of the autocrine ligand, $koff_{auto}$ is the dissociation rate constant of the autocrine ligand, $k_{eC}$ is the internalization rate constant for receptor/ligand complexes, $k_{eR}$ is the constitutive internalization rate constant, $k_{rec}$ is the rate of recycling, $k_{dgr}$ is the rate of degradation, fR is the fraction of receptors degraded, and Vs is the synthesis rate of receptors.

Once the above system of equations is solved, $f_{R\ occupied}$ is calculated based on occupied surface receptors, on total occupied receptors, and on a combination of surface and internal occupied receptors. We used Eq. 7 to combine surface occupied receptors with a fraction "*x*" of internal receptors to better fit our computational model to bulk medium experimental results.

$$f_{R\ occupied} = \frac{Cs_{auto} + x * Ci_{auto}}{Cs_{auto} + Rs + RiT} \quad [7]$$

Finally, to determine $f_{LC}$ from $f_{R\ occupied}$, we recognize that a balance must exist between the rate of ligand capture by cell

receptors and the rate of receptor binding by ligand (Eq. 8). Total ligand secretion rate, $V_{LT}$, and receptor appearance rate at the cell surface, $V_R$, were determined as described previously (DeWitt *et al.*, 2001).

$$f_{LC} * V_{LT} = f_{R\ occupied} * V_R \quad [8]$$

The value of "*x*" in Eq. 7 was estimated based on the closest visual match between experimental bulk medium conditioning results and our model output from Eq. 8, both in terms of $f_{LC}$, for the wild-type autocrine system; the best "*x*" was determined to be 0.6, whereas for the mutant autocrine system, it was determined to be 0.5. We attribute this difference to the lower receptor-binding affinity of the mutant ligand, which is expected to yield enhanced dissocation of the complex during endocytic trafficking (French and Lauffenburger, 1997).

## RESULTS

### *Computational Model for Autocrine Ligand Capture*

Previously, we reported that an important parameter governing autocrine ligand capture is the ratio of ligand production to receptor appearance, $V_{LT}/V_R$ (DeWitt *et al.*, 2001). Ligand production is equal to the total ligand secretion rate and is calculated from measurement of the concentration of EGF in the bulk medium when nearly all autocrine ligand appears in the medium (i.e., in the presence of excess blocking anti-EGFR mAb 225). Receptor appearance at the surface is due to both synthesis and recycling and is simply the number of surface receptors multiplied by the constitutive internalization rate constant when autocrine ligand production is negligible. We presented the fraction ligand capture ($f_{LC}$) and the fraction of occupied receptors ($f_{R\ occupied}$) as a function of this ratio for a WT EGF/EGFR autocrine system engineered into B82 mouse fibroblasts. Our data were obtained by using two experimental assays: first, a bulk medium conditioning assay indirectly measures $f_{LC}$ by measuring ligand escaping the producing cells; second, a Cytosensor microphysiometer assay measures the degree of receptor activation and, in combination with a computational microphysiometer model, permits calculation of $f_{R\ occupied}$. The measurements from these assays have been demonstrated to reflect the amount of ligand that is self-captured by producing cells before being lost to bulk medium by diffusion (Lauffenburger *et al.*, 1998).

These two quantities are related in that every EGF molecule captured by the cell results in an occupied EGFR, i.e., a simple rate balance (see Materials and Methods) can calculate $f_{LC}$ from $f_{R\ occupied}$, with $f_{R\ occupied}$ determined by using a computational autocrine cell model (see Materials and Methods). Two limiting cases exist for $f_{R\ occupied}$ calculations: the first considers total cell EGF/EGFR complexes, both internal and surface, while the second considers only surface complexes. $f_{R\ occupied}$ based on total complexes is always higher than $f_{R\ occupied}$ based on surface complexes because internal complexes arise from endocytosed surface complexes; occupied surface receptors have approximately a 10-fold enhancement in their internalization rate constant ($k_{eC}$ = 0.3 to 0.1 $min^{-1}$) over unoccupied receptors ($k_{eR}$ = 0.03 $min^{-1}$). When we use these two extreme values of $f_{R\ occupied}$ to calculate $f_{LC}$, we obtain predictions that should provide upper and lower limits for $f_{LC}$.

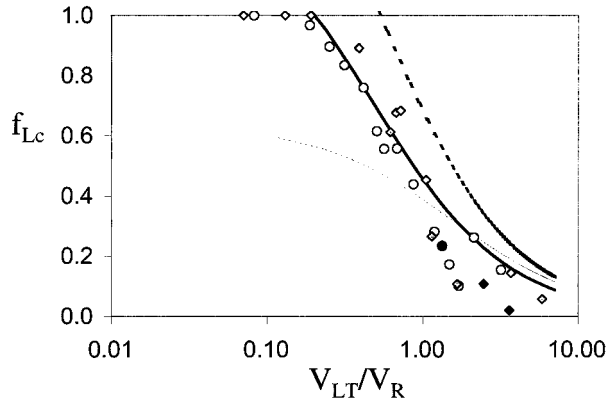


**FIG. 2.** Calculated fraction ligand capture from a computational model as a function of the production ratio agrees with experimentally measured fraction ligand capture. Using $f_{R\ occupied}$ results generated from a computational model and microphysiometer experimental data for the WT EGF/EGFR autocrine system (DeWitt *et al.*, 2001), we employed a kinetic rate balance (for ligand capture by receptors equalling receptor binding by ligand) to convert $f_{R\ occupied}$ to $f_{LC}$ for the wild-type autocrine system. Calculations were based on either total occupied receptors (dashed curve), surface occupied receptors (bold curve), or 100% surface complexes plus 60% internal complexes (dashed curve). The symbols are from bulk medium conditioning experimental results for this system (DeWitt *et al.*, 2001).

In Fig. 2, we can see that $f_{LC}$ decreases as the production ratio increases. $f_{LC}$ calculated with total complexes begins to decrease from unity at a production ratio of 0.5, while $f_{LC}$ calculated with surface complexes does not reach unity for any value of the production ratio. The points in Fig. 2 represent data previously reported for WT EGF capture as measured by bulk medium conditioning (DeWitt *et al.*, 2001). The two solutions from our autocrine computational model for the most part envelop, as they should, the results obtained from bulk medium conditioning experiments: model predictions derived from total receptors calculate a higher $f_{LC}$ for a given $V_{LT}/V_R$, and those derived from considering only surface receptors calculate a lower $f_{LC}$ compared with experimental results. This envelopment breaks down at high values of $V_{LT}/V_R$, where all receptors are essentially saturated; this happens because the endocytic internalization rate constant is assumed to be unchanging with occupied receptor number in the model, whereas in reality, the value of this parameter diminishes with increasing occupied receptor number (the phenomenon termed "saturation of internalization;" see Lauffenburger and Linderman, 1993). Because the ligand capture fraction is basically 0 at this point, however, this loss of model accuracy is not a significant problem.

To enable a unified prediction of the experimental data, we determined the combination of surface and internal complexes required to yield the measured signal. As shown by the dashed line model computation in Fig. 2, the combination of 100% of the surface complexes plus 60% of the internal complexes provides the best quantitative agreement with the experimental data (based on a residual minimization analysis). This comparison thus completely specifies all the parameters in our computational autocrine cell model from the WT EGF system, permitting *a priori* prediction of behavior as system parameters such as ligand/receptor binding affinity are varied.

### *Predictions for Effect of Binding Affinity on Autocrine Ligand Capture*

Given the complete specification of our computational autocrine cell model for the WT EGF autocrine system, we can now generate *a priori* predictions for the effect of changing the receptor/ligand binding affinity on $f_{LC}$ as a function of the ligand-to-receptor production ratio, $V_{LT}/V_R$. We use the model parameters determined above, changing only the binding constants. An important piece of the model computation is the linear relationship of effective local autocrine ligand concentration, $[L]_{auto}$, to ligand production rate, $V_{LT}$. We will prove later (see Fig. 5) that this same linear relationship holds for the low-affinity autocrine cells as for the WT autocrine cells. Thus, using the WT EGF system parameters, except with increasing dissociation rate constant (Fig. 3a) or decreasing association rate constant (Fig. 3b), the model predicts expected shifts in $f_{LC}$ vs $V_{LT}/V_R$. For a given binding equilibrium constant, a decrease in the association rate constant has a larger effect in decreasing a cell's capture efficiency than an equivalent increase in the dissociation rate constant; however, in both cases, for a decreased binding affinity, cells are predicted to be less efficient at capturing autocrine ligand. The difference between the WT and low-affinity curves is predicted to be significant, however, only for values of the ligand-to-receptor production rate ratio of $<1$; i.e., when ligand production is limiting for receptor binding (DeWitt *et al.*, 2001).

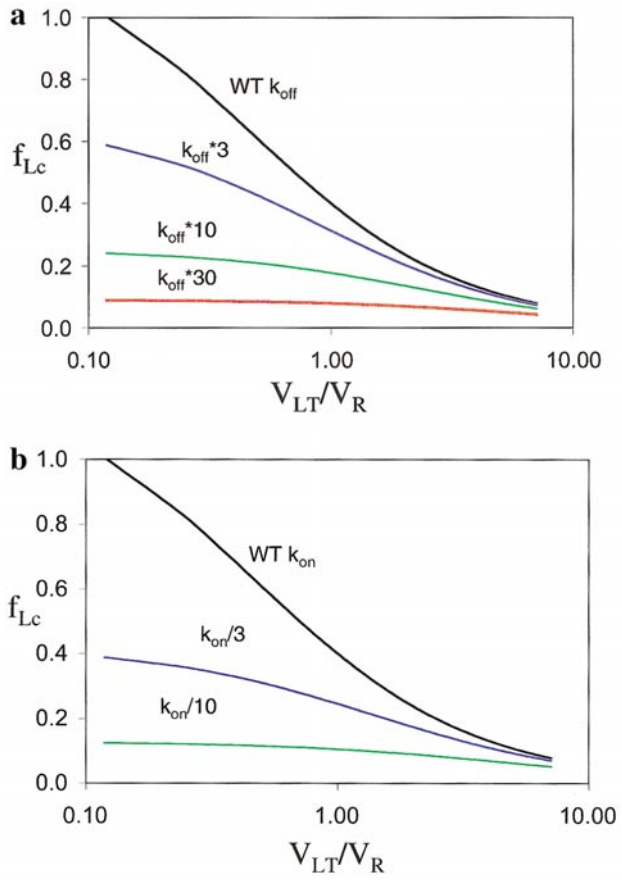


**FIG. 3.** Decreasing the binding affinity of an autocrine receptor/ligand pair decreases ligand capture efficiency in a manner dependent on whether the association or dissociation rate constant is altered. Using our computational model, $f_{LC}$ is predicted for EGF as a function of $V_{LT}/V_R$ based on the parameter specification for the WT EGF/EGFR system shown in Fig. 1, except across a ranges of values of autocrine ligand dissociation rate constant, $k_{off}$ (A), and association rate constant, $k_{on}$ (B).

### *Low-Affinity EGF Mutant Ligand Properties*

To experimentally test the model prediction that a low-affinity autocrine system is less efficient at capturing ligand than a higher affinity counterpart under ligand production-limiting conditions, we constructed a novel, low-affinity counterpart to our EGF/EGFR autocrine system. Several possibilities exist to alter the binding affinity of a receptor/ligand pair; and previous investigations indicated ways to alter the interaction of EGF for the hEGFR. Previous work has shown that Leu47 in the C-terminal region of EGF is important for high-affinity binding to the EGFR. Mutations of this residue from leucine to any of seven other amino acids (Ile, His, Pro, Ala, Gly, Asp, Arg) resulted in all mutations exhibiting a lower affinity to EGFR compared with wild-type (Matsunami *et al.*, 1991). AR studies also indicated the importance of residue 47 of EGF. AR binds to the EGFR with approximately a 10-fold lower affinity than EGF (Shoyab *et al.*, 1989). The mature form of AR does not have a leucine residue at the position analogous to position 47 of EGF; rather, AR has a methionine (Met86). Adam *et al.* (1995) found that modification of Met86 to Leu86 in a C-terminally extended AR construct increased the mitogenic potency nearly 2 orders of magnitude, corresponding to a possible increase in binding affinity to that of EGF for the EGFR.

With these investigations in mind, we created a low-affinity EGF/EGFR autocrine system by introducing a conservative mutation into EGF at residue 47; the leucine at residue 47 in wild-type EGF was converted to methionine. $EGF^{L47M}$ was then expressed in B82 EGFR+ cells, creating a new autocrine cell line. We then produced and purified

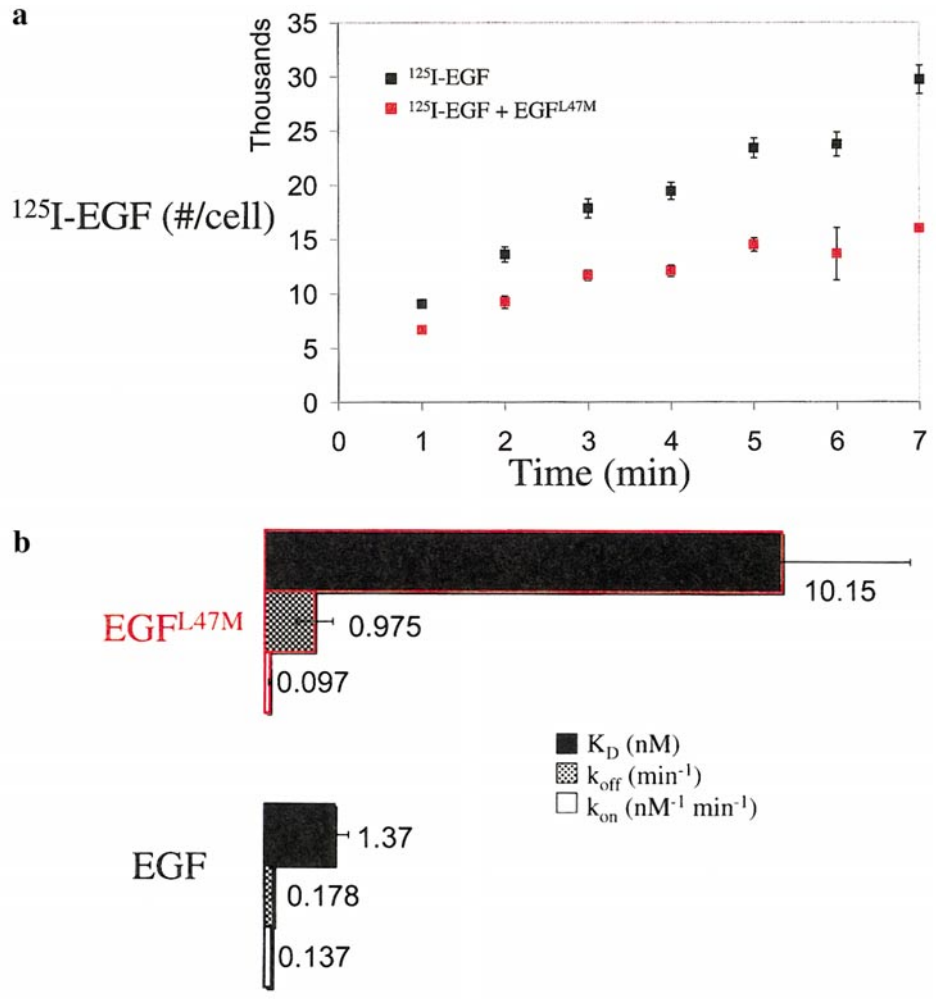


**FIG. 4.** (a) Fewer labeled complexes are formed at a given time when cold EGF$^{L47M}$ is added to medium containing $^{125}$I-EGF. B82 EGFR+ cells pretreated with 0.2 mM PAO were incubated with 1 nM $^{125}$I-EGF and with (red squares) or without (black squares) 10 nM EGF$^{L47M}$ for 1, 2, 3, 4, 5, 6, and 7 min in duplicate. The number of $^{125}$I-EGF molecules associated with the surface was collected and counted. (b) Binding affinity of EGF$^{L47M}$ is lower than EGF, primarily due to a change in the dissociation rate constant. Using five sets of data from radiolabeling experiments as presented in Fig. 3a, the association and dissociation rate constants of $^{125}$I-EGF and EGF$^{L47M}$ were calculated by using a nonlinear curve-fitting function.

EGF$^{L47M}$ for characterization using Chinese hamster ovary (CHO) cells. We used SDS-PAGE to confirm that EGF$^{L47M}$ has the same electrophoretic mobility as EGF, and thus the same approximate molecular weight. In addition, by visualizing polypeptide standards run in adjacent wells, both ligands appeared at the expected molecular weight, 6.2 kDa (results not shown).

We measured the association and dissociation rate constants of EGF$^{L47M}$ to the EGFR using competitive radiolabeling experiments. B82 EGFR+ cells were pretreated with PAO to inhibit internalization processes, and the rate constants were then calculated from data taken at 37°C. We ran two parallel sets of samples; the first set was challenged with only $^{125}$I-EGF, while the second set was challenged with $^{125}$I-EGF and cold EGF$^{L47M}$. We measured the number of $^{125}$I-EGF surface-associated counts in time. As we would expect, EGF$^{L47M}$ competes with $^{125}$I-EGF for binding to the EGFR; therefore, samples containing cold EGF$^{L47M}$ and $^{125}$I-EGF render low counts than those with only $^{125}$I-EGF as shown in Fig. 4a. Using five data sets, we used a nonlinear curve fitting function to calculate the association and dissociation rate constants for $^{125}$I-EGF and EGF$^{L47M}$.

As shown in Fig. 4b, the values calculated for the association rate constants of $^{125}$I-EGF and EGF$^{L47M}$ are 0.14 and 0.097 nM$^{-1}$ min$^{-1}$, respectively; dissociation rate constants are 0.18 and 0.98 min$^{-1}$ respectively. Kinetic rate constants for $^{125}$I-EGF have been previously reported in literature, and our values for EGF agree well with those reported, $k_{on}$ (nM$^{-1}$

$min^{-1}$) = 0.063 ± 0.02, $k_{off}$ ($min^{-1}$) = 0.16 ± 0.05 for EGF (French *et al.*, 1995). While the association rate constants we measured for EGF and $EGF^{L47M}$ are relatively close, the dissociation rate constants are noticeably different. The dissociation rate constant of $EGF^{L47M}$ is considerably larger than that of EGF, leading to approximately an eightfold decrease in the binding affinity of $EGF^{L47M}$ ($K_D$ = 10 nM) for the EGFR compared with wild-type EGF ($K_D$ = 1.3 nM).

### *Model Predictions and Experimental Test Using $EGF^{L47M}$ Autocrine System*

As noted earlier, our model predictions require that the linear relationship between $L_{auto}$ and $V_{LT}$ discerned from wild-type EGF microphysiometer data analysis holds for the low-affinity EGF mutant system. We now validate this by applying the same analysis to microphysiometer data collected using low-affinity autocrine cells as we did previously to our wild-type autocrine system (Appendix B in DeWitt *et al.*, 2001) to generate $L_{auto}$ vs $V_{LT}$ for our low-affinity system. We expect that the relationship between $L_{auto}$ and $V_{LT}$ should be the same for both wild-type and low-affinity systems, that is, the concentration of autocrine ligand is only a function of the ligand secretion rate. Fig. 5 shows that the slopes of $L_{auto}$ vs $V_{LT}$ calculated using wild-type and low-affinity ligand-producing cells are statistically equivalent; the best-fit individual slope values are 0.0036 ± 0.0001 and 0.0045 ± 0.0010, respectively, and the hypothesis of equivalent slopes was not rejected ($P > 0.65$) by ANOVA. The mutant ligand-producing cells exhibit greater variance in their behavior here than do the wild-type ligand-producing cells, because the latter were clonal with tet-off system for regulating ligand synthesis, whereas the former were generated from different clones. Also, the mutant ligand-producing cells appeared to be limited by their particular promoter in the ligand synthesis rate they were capable of generating. This result validates our use of this relationship to predict the effects of altering binding affinity on fraction receptors occupied and thus fraction ligand captured.

To now specifically test our model predictions for the $EGF^{L47M}$/EGFR autocrine system, to compare the computational results with the experimental data on local ligand capture as a function of the production ratio for these cells (Fig. 6). The black dashed line and black points corresponding to the wild-type EGF situation are repeated from Fig. 2, recalling the best-fit obtained with signaling from 60% of the internalized ligand/receptor complexes. The red points in Fig. 6 correspond to the mutant EGF situation, with the two red dashed curves representing the model predictions for 60 and 50% intracellular complex signaling; for this ligand, 50% provides a better fit, likely arising from the enhancement of ligand/receptor complex dissociation during endocytosis for the lower-affinity ligand (French and Lauffenburger, 1997). With this reasonable single-parameter modulation, the model predictions are borne out by the data, both showing that the low-affinity EGF mutant is locally captured less efficiently as long as the ligand-to-receptor production ratio is less than unity.

Consider, for instance, a ligand/receptor production ratio, $V_{LT}/V_R$, of 0.3. For wild-type EGF binding affinity, less than 10% of the released ligand escapes proximal capture, whereas for the roughly eightfold lower $EGF^{L47M}$ binding affinity, more than 50% escapes local capture. Although this disparity for our specific $EGF^{L47M}$ case may not seem major, reference to Fig. 2 makes clear that very large differences in local capture fraction can occur for greater changes in affinity.

## DISCUSSION

In this work, we have determined how the ability of cells to locally capture autocrine ligands can be influenced by receptor-binding affinity. We have accomplished this by comparing the local capture of wild-type EGF ($K_D$ = 1.3 nM) vs an $EGF^{L47M}$ mutant ($K_D$ = 10 nM) produced as autocrine factors in EGFR-expressing B82 cells, employing a combination of ELISA and microphysiometer measurements in the absence and presence of an anti-EGFR-blocking antibody at saturating concentration and for varying levels of ligand and receptor expression. ELISA measures the fraction of ligand escaping capture by EGFR binding, while the microphysiometer measures the fraction of EGFR binding ligand (Oehrtman *et al.*, 1998; Lauffenburger *et al.*, 1998; DeWitt *et al.*, 2001); together, these two assays, along with independent evaluation of the key rate constants for binding and endocytic trafficking, enable validation of a computational model for autocrine ligand capture dynamics.

The model predicts, and our experimental data for wild-type EGF confirms, that an important quantity governing the fraction of locally captured autocrine ligand is the ratio of the rate of ligand secretion, $V_{LT}$, to the rate of receptor appearance on the cell surface (via both new synthesis and endocytic recycling), $V_R$. As can be seen in Fig. 2, local capture is near 1 for low values of this ratio and diminishes to near 0 for high values of this ratio. When the ligand production rate is too great relative to the rate at which receptors arrive on the cell plasma membrane, the receptors quickly become saturated so that most of the additional ligand diffuses away to more distal locations, as illustrated in Fig. 1. Basically, the system can transition between operating in predominantly autocrine mode (the fraction locally captured near 1) to predominantly paracrine mode (the fraction locally captured near 0), depending on the value of $V_{LT}/V_R$.

The central question of our work here, then, is how the value of ligand/receptor binding affinity, $K_D$, influences local autocrine factor capture; i.e., whether the system is operating mainly in autocrine or paracrine mode. The computational model predicts that for lower affinity ligand, the fraction locally captured should be diminished—but only when the ratio $V_{LT}/V_R$ is sufficiently small. Our experimental data for our EGF B82 cell system here, as seen in Fig. 6, confirm this prediction. Indeed, there exists a

window of ratios of ligand-to-receptor production rates in which a reduction in ligand/receptor binding affinity leads to reduction in local autocrine capture. Another way to look at this is that the position of the curve of local ligand capture as a function of $V_{LT}/V_R$ varies with the value of $K_D$; for increasing $K_D$ (lower binding affinity), this curve shifts to the left. In our experimental system here, comparing wild-type EGF and the $EGF^{L47M}$ mutation, the difference in $K_D$ values is only approximately eightfold, so that the shift is significant but not large; the change in the value of the ratio $V_{LT}/V_R$ for which 50% of the produced ligand is captured locally changes by roughly four-fold. The model predicts that more quantitatively dramatic changes should be found for greater differences in $K_D$ values. One can infer, accordingly, that for similar ligand production rates, a high-affinity ligand system may operate in mainly autocrine mode, while a low-affinity ligand system may be operating in mainly paracrine mode.

This work has been motivated by the myriad roles of autocrine ligand/receptor loops in embryonic development and tissue organization, especially in regard to the EGFR system (Freeman, 1996; Newman and Sternberg, 1996; Van Buskirk and Schupbach, 1999; Freeman, 2000), as well as in pathological dysregulation (Casci and Freeman, 1999). Because quantitative changes in molecular and cellular properties can lead to qualitative alterations in phenotypic behavior, it is important to pursue quantitative understanding of the effects molecular and cellular parameters on operation of the EGFR autocrine system. As one example, in *Drosophila* oogeensis, DER-mediated pattern formation by a network of stimulatory and inhibitory autocrine loops induces the formation of respiratory appendages on the dorsal side of the eggshell. This patterning can be strongly governed by the comparative spatial ranges of the secreted Spitz and Argos DER ligands (Wasserman and Freeman, 1998; Shvartsman *et al.*, 2002). A variety of properties have been theoretically proposed to influence the distance of ligand diffusion before capture by cell receptor binding, including ligand effective diffusivity through the extracellular matrix (potentially affected by ligand/matrix interactions); ligand/receptor binding affinity, and ligand/receptor endocytic internalization and recycling rates (Chu *et al.*, 1996; Strigini and Cohen, 1999; Shvartsman *et al.*, 2001; Teleman *et al.*, 2001; Lander *et al.*, 2002). However, none of these properties has previously been investigated for its actual effects on autocrine ligand spatial localization. Our findings that receptor-binding affinity can, in fact, help govern the ability of cells to capture autocrine ligand locally are thus novel. At first look, the reduction in local ligand capture for a lower-affinity ligand seems straightforward—but, as can be seen in Fig. 6, this molecular-property effect turns out to strongly depend on a cellular-property effect: that of the ligand-vs-receptor appearance rates ratio. This means that the extent to which receptor binding affinity regulates autocrine ligand spatial localization may vary with cell expression levels of both ligand and receptor as well as other processes, such as endocytic trafficking, that influence cell receptor levels. Therefore, different investigators may observe diverse results for such a question—or even a deceivingly simple question such as whether a given ligand/receptor pair is operating in autocrine mode or paracrine mode—depending on their system of study and even confounding protocol conditions for a given system. It is important to understand the multivariable nature of this complicated dynamic phenomenon for proper intepretation of experimental findings, hence our aim of validating predictions of a computational model in which many key features of the phenomenon are represented.

Concerning the DER/Spitz/Argos system in particular, it is not clear whether the literature reports of highly localized Spitz effects in contrast to the more distal Argos influence (e.g., Stemerdink and Jacobs, 1997; Gabay *et al.*, 1997; Bergmann *et al.*, 2002) are necessarily due to Argos possessing lower DER-binding affinity. Experimental studies of Spitz and Argos binding have given mixed results. Jin *et al.* (2000) found that the $K_D$ values for Argos and Spitz binding to DER immobilized on a BIACore biosensor chip are roughly similar, with the Argos value actually perhaps a bit smaller; van de Poll *et al.* (1997), on the other hand, found that an engineered Argos-like EGF mutant binds to cell surface EGFR with lower affinity. Thus, it may well be the case that the disparity in Spitz-vs-Argos spatial localization of DER binding in *Drosophila* embryos arises from currently unexamined differences among one or more of the alternative properties such as diffusivity or trafficking. In mammalian tissue organization, where AR, TGF$\alpha$, and EGF effects show distinctions (Snedeker *et al.*, 1991; Herrington *et al.*, 1997; Luettke *et al.*, 1999), EGFR binding and trafficking property differences among these autocrine ligands are known (Shoyab *et al.*, 1989; Derynck, 1992; French *et al.* 1995).

Our experimental assays are able to measure proximal capture of ligand by producing cells. Both the ELISA and microphysiometer setups involve cell monolayers, at slightly subconfluent densities, on horizontal two-dimensional surfaces. The volumes of bulk media above these surface are sufficiently vast that once ligand escapes cell receptor capture by significant diffusion into the vertical, third dimension its probability of returning for later capture is extremely small within the experimental assay time periods (Forsten and Lauffenburger, 1994; Shvartsman *et al.*, 2001). And, because the probability of diffusion into the vertical third dimension is similar to that of diffusion across the horizontal two-dimensional surface, it is highly likely that the ligand will escape into the bulk media before traversing more than a very small number cells adjacent to the producing cell (Forsten and Lauffenburger, 1994; Shvartsman *et al.*, 2001). Thus, although we cannot be certain that our assays determine whether any particular ligand molecule is captured by the very cell that produced it, we believe that they determine, within reasonable accuracy, the fraction of ligand molecules which captured by either the producing cell itself or a proximal neighbor. This assumption is validated by our previous experimental work

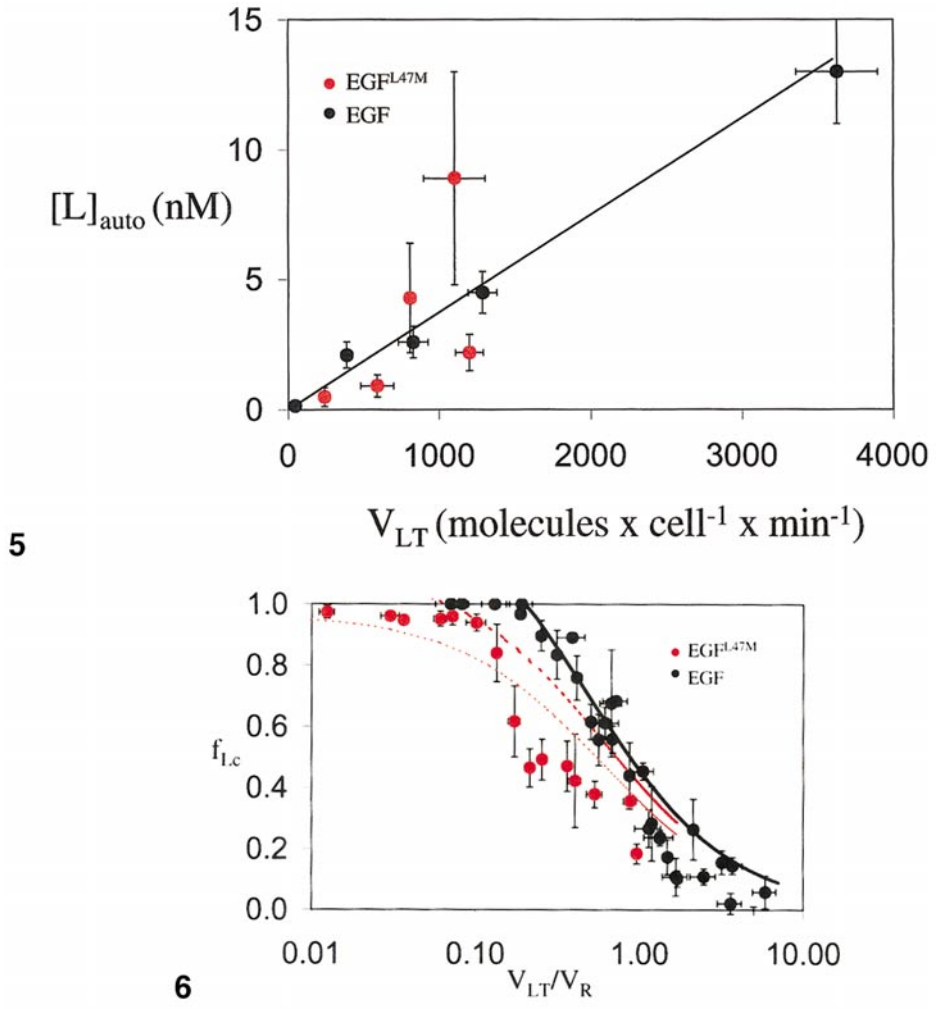


**FIG. 5.** Autocrine ligand concentration is a function of total ligand secretion rate and is not dependent on ligand/receptor binding affinity. Using microphysiometer $EGF^{L47M}$ autocrine cell data, the effective autocrine ligand concentration, $[L]_{auto}$, was determined as a function of total ligand secretion rate, $V_{LT}$ (DeWitt *et al.*, 2001). The total ligand secretion rate was measured in parallel by the bulk medium conditioning assay. Red circles represent $EGF^{L47M}$, while black circles represent WT EGF. The best-fit slope for the combined data, 0.0037 ± 0.0004, is statistically equivalent to the individual best-fit slopes for each data set separately (wild-type: 0.0036 ± 0.0001; mutant: 0.0045 ± 0.0010).

**FIG. 6.** For values of the ligand-to-receptor production ratio, $V_{LT}/V_R$, <1, $EGF^{L47M}$ autocrine ligand is locally captured less efficiently than WT EGF. Computational model predictions for the fraction of autocrine ligand captured locally, $f_{LC}$ are shown for $EGF^{L47M}$ by the red dashed curve (small dashes correspond to 50% intracellular complex signaling; large dashes correspond to 60% intracellular complex signaling), and are experimentally confirmed by the data for $EGF^{L47M}$ (red circles). Results for WT EGF from Fig. 2 are provided for comparison [black circles, data; black dashed curve corresponds to 60% intracellular complex signaling (see text)].

demonstrating that anti-ligand "decoy" antibodies are much less effective in interrupting autocrine signaling loops than are anti-receptor "blocking" antibodies (Lauffenburger *et al.*, 1998).

Our current assays do not, however, measure the actual distance traversed by a ligand between production and capture (although theoretical relationships between the escape fraction and travel distance can be derived; Shvartsman *et al.*, 2001). This would most precisely require a method for following a particular ligand trajectory. Surrogate information could be obtained, at least in an averaged sense, by observing the formation of gradients in ligand and bound cell receptors in a three-dimensional matrix (in order to minimize escape into a non binding third dimension from a two-dimensional cell monolayer). This is the type of experiment which has been employed in study of morphogen behavior in developmental biology (e.g., see Jessell and Melton, 1992; Teleman *et al.*, 2001; Vincent and Briscoe, 2001). With relatively few exceptions, these kinds of studies have focused on paracrine ligands and how they travel from

producing cells to receiving cells; interpretation of the experimentally observed ligand distributions is not simple (Lander *et al.*, 2002). The situation we study here, that of potential autocrine operation in which the ligand-producing cells traversed express receptors for the ligand, is more complicated yet. At the same time, autocrine signaling loops inherently possess exceptional opportunity for regulation of tissue organization (Freeman, 2000), so that our first steps here toward improved quantitative understanding may prove helpful as the number of such systems identified in developmental applications continues to grow.

## ACKNOWLEDGMENTS

This work has been partially funded by NIH grants GM62575 and HD28528. Helpful discussions with Stanislav Shvartsman are also gratefully acknowledged.

## REFERENCES

Adam, R., Drummond, D. R., Solic, N., Holt, S. J., Sharma, R. P., Chamberlin, S. G., and Davies, D. E. (1995). Modulation of the receptor-binding affinity of amphiregulin by modification of its carboxyl-terminal tail. *Biochim. Biophys. Acta* **1266,** 83–90.

Baonza, A., Casci, T., and Freeman, M. (2001). A primary role for the EGF receptor in ommatidial spacing in the *Drosophila* eye. *Curr. Biol.* **11,** 398–404.

Bersgmann, A., Tugentman, M., Shilo, B. Z., and Steller, H. (2002). Regulation of cell number by MAPK-dependent control of apoptosis: A mechanism for trophic survival signaling. *Dev. Cell* **2,** 159–170.

Bier, E. (1998). Localized activation of RTK/MAPK pathways during *Drosophila* development. *Bioessays* **20,** 189–194.

Casci, T., and Freeman, M. (1999). Control of EGF receptor signalling: Lessons from fruitflies. *Cancer Metastasis Rev.* **18,** 181–201.

Chang, C., Newman, A. P., and Sternberg, P. W. (1999). Reciprocal EGF signaling back to the uterus from the induced *C. elegans* vulva coordinates morphogenesis of epithelia. *Curr. Biol.* **9,** 237–246.

Chu, L., Wiley, H. S., and Lauffenburger, D. A. (1996). Endocytic relay as a potential means for enhancing ligand transport through cellular tissue matrices. *Tissue Eng.* **2,** 17–38.

Chung, E. K., and Coffey, R. J. (2000). Multiple forms of secreted amphiregulin exhibit differential EGF receptor binding. *Mol. Biol. Cell* **11,** 146.

Chung, Y. H., Kim, J. A., Song, B. C., Lee, G. C., Koh, M. S., Lee, Y. S., Lee, S. G., and Suh, D. J. (2000). Expression of TGF$\alpha$ mRNA in livers of patients with chronic viral hepatitis and hepatocellular carcinoma. *Cancer* **89,** 977–982.

Derynck, R. (1992). The physiology of TGF$\alpha$. *Adv. Cancer Res.* **5,** 27–53.

DeWitt, A. E., Dong, J. Y., Wiley, H. S., and Lauffenburger, D. A. (2001). Quantitative analysis of the EGF receptor autocrine system reveals cryptic regulation of cell response by ligand capture. *J. Cell Sci.* **114,** 2301–2313.

Forsten, K. E., and Lauffenburger, D. A. (1994). Probability of autocrine ligand capture by cell-surface receptors: Implications for ligand secretion measuremetns. *J. Comp. Biol.* **1,** 15–23.

Freeman, M. (1996). Reiterative use of the EGF receptor triggers differentiation of all cell types in the *Drosophila* eye. *Cell* **87,** 651–660.

Freeman, M. (1997). Cell determination strategies in the *Drosophila* eye. *Development* **124,** 261–270.

Freeman, M. (2000). Feedback control of intercellular signalling in development. *Nature* **408,** 313–319.

French, A. R., and Lauffenburger, D. A. (1997). Controlling receptor/ligand trafficking: Effects of cellular and molecular properties on endosomal sorting. *Ann. Biomed. Eng.* **25,** 690–707.

French, A. R., Tadaki, D. K., Niyogi, S. K., and Lauffenburger, D. A. (1995). Intracellular trafficking of EGF family ligands is directly influenced by the pH sensitivity of the receptor-ligand interaction. *J. Biol. Chem.* **270,** 4334–4340.

Gabay, L., Seger, R., and Shilo, B. Z. (1997). *In situ* activation pattern of *Drosophila* EGF receptor pathway during development. *Science* **277,** 1103–1106.

Gibson, A. E., Noel, R. J., Herlihy, J. T., and Ward, W. F. (1989). Phenylarsine oxide inhibition of endocytosis: Effects on asialofetuin internalization. *Am. J. Physiol.* **257,** C182–C184.

Golembo, M., Raz, E., and Shilo, B. Z. (1996). The *Drosophila* embryonic midline is the site of Spitz processing, and induces activation of the EGF receptor in the ventral ectoderm. *Development* **122,** 3363–3370.

Herrington, E. E., Ram, T. G., Salomon, D. S., Johnson, G. R., Gullick, W. J., Kenney, N., and Hosick, H. L. (1997). Expression of EGF-related proteins in the aged adult mouse mammary gland and their relationship to tumorigenesis. *J. Cell Physiol.* **170,** 47–56.

Hisaka, T., Yano, H., Haramaki, M., Utsunomiya, I., and Kojiro, M. (1999). Expressions of epidermal growth factor family and its receptor in hepatocellular carcinoma cell lines: relationship to cell proliferation. *Int. J. Oncol.* **14,** 453–460.

Horvitz, H. R., and Sternberg, P. W. (1991). Multiple intercellular signaling systems control the development of the *Caenorhabditis elegans* vulva. *Nature* **351,** 535–541.

Iwamoto, R., and Makeda, E. (2000). Heparin-binding EGF-like growth factor: a juxtacrine growth factor. *Cyt. Growth Factor Rev.* **11,** 335–344.

Jessell, T. M., and Melton, D. A. (1992). Diffusible factors in vertebrate embryonic induction. *Cell* **68,** 257–270.

Jin, M.-H., Sawamoto, K., Ito, M., and Okano, H. (2000). The interaction between the *Drosophila* secreted protein Argos and the EGF receptor inhibits dimerization of the receptor and binding of secreted Spitz to the receptor. *Mol. Cell. Biol.* **20,** 2098–2107.

Kim, H. G., Kassis, J., Souto, J. C., Turner, T., and Wells, A. (1999). EGF receptor signaling in prostate morphogenesis and tumorigenesis. *Histol. Histopathol.* **14,** 1175–1182.

Klambt, C. (2002). EGF receptor signaling: Roles of Star and Rhomboid revealed. *Curr. Biol.* **12,** R21–R23.

Kornfeld, K. (1997). Vulval development in *Caenorhabditis elegans. Trends Genet.* **13,** 55–61.

Lander, A. D., Nie, Q., and Wan, F. Y. M. (2002). Do morphogen gradients arise by diffusion? *Dev. Cell* **2,** 785–796.

Lauffenburger, D. A., and Linderman, J. J. (1993). "Receptors: Models for Binding, Trafficking, and Signaling". Oxford University Press.

Lauffenburger, D. A., Oehrtman, G. T., Walker, L., and Wiley, H. S. (1998). Real-time quantitative measurement of autocrine ligand binding indicates that autocrine loops are spatially localized. *Proc. Natl. Acad. Sci. USA* **95,** 15368–15373.

Li, S. W., Plowman, G. D., Buckley, S. D., and Shipley, G. D. (1992). Heparin inhibition of autonomous growth implicates amphiregulin as an autocrine growth factor for normal human mammary epithelial cells. *J. Cell Physiol.* **153,** 103–111.

Luettke, N. C., Qiu, T. H., Fenton, S. E., Troyer, K. L., Riedel, R. F., Chang, A., and Lee, D. C. (1999). Targeted inactivation of the EGR and AR genes reveals distinct roles for EGF receptor ligands in mouse mammary gland development. *Development* **126,** 2739–2750.

Matsunami, R. K., Yette, M. L., Stevens, A., and Niyogi, S. K. (1991). Mutational analysis of leucine-47 in human EGF. *J. Cell Biochem.* **46,** 242–249.

Miettinen, P. J., Chin, J. R., Shum, L., Slavkin, H. C., Shuler, C. F., Derynck, R., and Werb, Z. (1999). EGF receptor function is necessary for normal craniofacial development and palate closure. *Nat. Genet.* **22,** 69–73.

Moghal, N., and Sternberg, P. W. (1999). Multiple positive and negative regulators of signaling by the EGF receptor. *Curr. Opin. Cell Biol.* **11,** 190–196.

Newman, A. P., and Sternberg, P. W. (1996). Coordinated morphogenesis of epithelia during development of the Caenorhabditis elegans uterine–vulval connection. *Proc. Natl. Acad. Sci. USA* **93,** 9329–9333.

Oehrtman, G. T., Wiley, H. S., and Lauffenburger, D. A. (1998). Escape of autocrine ligands into extracellular medium: Experimental test of theoretical model predictions. *Biotechnol. Bioeng.* **57,** 571–582.

Panico, L., Dantonio, A., Salvatore, G., Mezza, E., Tortora, G., DeLaurentiis, M., DePlacido, S., Giordano, T., Merino, M., Salomon, D. S., Mullick, W. J., Pettinato, G., Schnitt, S. J., Bianco, A. R., and Ciardiello, F. (1996). Differential immunohistochemical detection of TGF$\alpha$, amphiregulin and CRIPTO in human normal and malignant breast tissues. *Int. J. Cancer* **65,** 51–56.

Piepkorn, M., Pittelkow, M. R., and Cook, P. W. (1998). Autocrine regulation of keratinocytes: The emerging role of heparin-binding, epidermal growth factor-related growth factors. *J. Invest. Dermatol.* **111,** 715–721.

Russell, W. E., Dempsey, P. J., Sitaric, S., Peck, A. J., and Coffey, R. J. (1993). Transforming growth factor-alpha concentrations increase in regenerating rat liver: evidence for a delayed accumulation of mature TGF$\alpha$. *Endocrinology* **133,** 1731–1738.

Schroeder, J. A., and Lee, D. C. (1998). Dynamic expression and activation of ErbB receptors in the developing mouse mammary gland. *Cell Growth Differ.* **9,** 451–464.

Schweitzer, R., Howes, R., Smith, R., Shilo, B. Z., and Freeman, M. (1995). Inhbition of *Drosophila* EGF receptor activation by secreted protein Argos. *Nature* **376,** 699–702.

Schweitzer, R., and Shilo, B. Z. (1997). A thousand and one roles for the *Drosophila* EGF receptor. *Trends Genet.* **13,** 191–196.

Shoyab, M., Plowman, G. D., McDonald, V. L., Bradley, J. G., and Todaro, G. J. (1989). Structure and function of human amphiregulin: A member of the EGF family. *Science* **243,** 1074–1076.

Shvartsman, S. Y., Wiley, H. S., Deen, W. M., and Lauffenburger, D. A. (2001). Spatial range of autocrine signaling: Modeling and computational analysis. *Biophys. J.* **81,** 1854–1867.

Shvartsman, S. Y., Muratov, C. B., and Lauffenburger, D. A. (2002). Modeling and computational analysis of EGF receptor-mediated cell communication in *Drosophila* oogenesis. *Development* **129,** 2577–2589.

Snedeker, S. M., Brown, C. F., and DiAugustine, R. P. (1991). Expression and funcational properties of TGF$\alpha$ and EGF during mouse mammary gland ductal morphogenesis. *Proc. Natl. Acad. Sci. USA* **88,** 276–280.

Stemerdink, C., and Jacobs, J. R. (1997). Argos and Spitz group genes function to regulate midline glial cell number in *Drosophila* embryos. *Development* **124,** 3787–3796.

Strigini, M., and Cohen, S. M. (1999). Formation of morphogen gradients in the *Drosophila* wing. *Semin. Cell Dev. Biol.* **10,** 335–344.

Teleman, A. A., Strigini, M., and Cohen, S. M. (2001). Shaping morphogen gradients. *Cell* **105,** 559–562.

Van Buskirk, C., and Schupbach, T. (1999). Versatility in signalling: Multiple responses to EGF receptor activation during *Drosophila* oogenesis. *Trends Cell Biol.* **9,** 1–4.

van de Poll, M. L., van Vugt, M. J., Lenferink, A. E., and van Zoelen, E. J. (1997). Insertion of Argos sequences into the B-loop of EGF results in a low-affinity ligand with strong agonistic activity. *Biochemistry* **36,** 7425–7431.

Vincent, J.-P., and Briscoe, J. (2001). Morphogens. *Curr. Biol.* **11,** R851–R854.

Wasserman, J. D., and Freeman, M. (1997). Control of EGF receptor activation in *Drosophila. Trends Cell Biol.* **7,** 431–436.

Wasserman, J. D., and Freeman, M. (1998). An autoregulatory cascade of EGF receptor signaling patterns the *Drosophila* egg. *Cell* **95,** 355–364.

Wiesen, J. F., Young, P., Werb, Z., and Cunha, G. R. (1999). Signaling through the stromal EGF receptor is necessary for mammary ductal development. *Development* **126,** 335–344.

Wiley, H. S., Woolf, M. F., Opresko, L. K., Burke, P. M., Will, B., Morgan, J. R., and Lauffenburger, D. A. (1998). Removal of the membrane-anchoring domain of EGF leads to intracrine signaling and disruption of mammary epithelial cell organization. *J. Cell Biol.* **143,** 1317–1328.

Will, B., Lauffenburger, D. A., and Wiley, H. S. (1995). Studies on engineering autocrine systems: Requirements for ligand release from cells producing an artifical growth factor. *Tissue Eng.* **1,** 81–94.

Yarden, Y. (2001). The EGF receptor family and its ligands in human cancer: Signalling mechanisms and therapeutic opportunities. *Eur. J. Cancer* **37,** S3–S8.

Received for publication January 7, 2002
Revised July 11, 2002
Accepted August 1, 2002
Published online September 12, 2002